

Article

# Seasonal Dynamics of Stem Radial Increment of *Pinus taiwanensis* Hayata and Its Response to Environmental Factors in the Lushan Mountains, Southeastern China

Xinsheng Liu <sup>1,\*</sup> , Yuqin Nie <sup>1</sup> and Feng Wen <sup>2</sup>

<sup>1</sup> College of Tourism and Territorial Resources, Jiujiang University, East Qianjin Road No. 551, Jiujiang 332005, China; nieyq1224@163.com

<sup>2</sup> College of Pharmacy and Life Science, Jiujiang University, Jiujiang 332005, China; wenfeng332@126.com

\* Correspondence: xslu287@gmail.com

Received: 14 May 2018; Accepted: 26 June 2018; Published: 29 June 2018



**Abstract:** Seasonal radial-increment records can help to elucidate how tree growth responds to climate seasonality. Such knowledge is critical for understanding the complex growth-climate relationships in subtropical China. We hypothesize that under subtropical monsoon climate characterized by mild winters and hot summers, summer drought constrains stem radial increment, which generally results in growth-limiting factors switching from temperatures in spring and early summer to precipitation in summer and autumn. Here, we monitored intra-annual dynamics of stem radial increment with band dendrometers in a montane stand of Taiwan pine (*Pinus taiwanensis* Hayata) from Lushan Mountains for two consecutive years (2016–2017). A pronounced bimodal seasonal pattern of stem radial increment was observed in 2016. However, it was less clear in 2017 when late-summer rainfall events occurred in early August. Changing growth-climate relationships were detected throughout the two growing seasons. Stem increments were consistently positively correlated with temperatures before early July, whereas the growth-temperature dependency was gradually weakened and more variable after early July. Conversely, stem increments were significantly correlated with precipitation and soil moisture since early July, indicating that moisture variables were the main factor limiting stem increments in dry period. More precipitation was received in the dry period (July–November) of 2017 as compared with the year 2016, which favoured a wider annual increment in 2017, although growing-season temperature and precipitation was similar between years. Our study suggests a seasonal shift in growth-limiting factors in subtropical forests, which should be explicitly considered in forecasting responses of tree growth to climatic warming.

**Keywords:** *Pinus taiwanensis* Hayata; automatic dendrometer; stem increment; summer drought; subtropical China

## 1. Introduction

Forest ecosystems, the largest component of the terrestrial biosphere, play a critical role in regulating carbon and water exchanges of the soil-plant-atmosphere continuum [1]. Tree growth can persistently sequester carbon through biomass formation, which is a major contributor to the terrestrial carbon sink [2]. There is increasing evidence that climate change can exert considerable influences on tree growth and forest productivity, but the directionality (positive or negative effects) of these changes is largely dependent on site conditions and tree species [3,4]. Although the knowledge of climatic forcing of tree growth has been intensively documented in mid-to-high latitudes [5–8], studies in the

subtropical regions are still rare. Thus, information on growth-climate relationships is urgently needed to improve our understanding of subtropical forest response to future climate change.

As one of the principal carbon uptakes of global forests [9], the subtropical forests in south China are currently subjected to climate-warming induced multiple threats, including rising air temperature and increased frequency and intensity of summer drought [10]. Generally, temperature-limited trees in cold climates responded positively to changes in temperature [5,11], whereas negative effects of deficits in precipitation and increased evaporative demand under warmer temperatures on tree growth were observed in water-limited forests [8,12]. However, previous dendroclimatological studies showed ambivalent responses of tree growth to climate change in south China, including increases in tree growth under warmer springs and tree growth decline owing to summer droughts [13–16]. These contrasting tree growth responses clearly suggest that there is a complex growth-climate relationship in subtropical forests [17]. It should be noted that current understandings mostly rely on investigating the correlations between annual ring width series and monthly, seasonal and annual climate variables, which may not truly capture the seasonal growth variability and growth-limiting factors, as annual tree-ring formation is a highly dynamic process [18]. To mechanistically elucidate the environmental variables driving tree growth, fine time scales ranging from days to weeks are required.

Automatic dendrometers, which continuously record stem radius variations with a sub-daily resolution, have been recognized as a useful tool for measuring stem radial growth [19–23]. Physiologically, diurnal stem radius variations consist of two main components, which is irreversible growth of new xylem cells as well as reversible stem shrinkage and swelling associated with water balance within the stems [21,22,24]. It has been demonstrated that tree growth can be reliably separated from the diurnal stem radius variations through conceptual partitioning approaches [20–22,25], providing a general basis for quantifying intra-annual tree growth and its association with climate and soil characteristics across coniferous and broadleaf trees from different biomes [20,26–29]. A number of recent studies used this technique to monitor intra-annual tree growth and evaluated the climate-growth relationships of temperate and tropical forests in China [28,30,31]. To date, the observation of seasonal stem growth dynamics is still sparse in subtropical China [32], rendering the climatic forcing of tree growth unknown. Moreover, a stable correlation between tree growth and climate was generally assumed throughout the entire growing season (e.g., [28,29,33]), without explicitly considering the seasonal variability in growth response to changing environmental constraints. It has been demonstrated that hot summers could induce a negative effect on fine-scale stem growth of temperate tree species [34]. However, no attention has been paid to the seasonal variations in growth-climate relationships of subtropical trees, where summer droughts caused by high temperature together with low rainfall periodically occur in this region. Such knowledge is important in the search for a general explanation for the complex growth-climate relationships of subtropical forests in south China.

Taiwan pine (*Pinus taiwanensis* Hayata) is an endemic conifer species and is widespread on mountain areas in southeast China [35]. In the Lushan Mountains, Taiwan pine widely dominate at the highlands ranging from 800 to 1460 m. Several dendroclimatological studies of Taiwan pine have been conducted in southeast China, but contradictory climatic limiting factors including winter temperature [13], spring-early summer temperature [36,37] and previous growing-season temperature [38] were reported. Also, there was no significant correlation between tree growth and precipitation in the above studies. To our knowledge, growth-climate relationships of Taiwan pine at fine time scales still remain unexamined in subtropical China. Here, we monitored the daily stem radius variations of Taiwan pine and relevant meteorology data in the Lushan Mountains over two consecutive years. We tested the hypothesis that summer drought constrains stem radial increment, resulting in a seasonal shift in growth-limiting factors in subtropical forests. Specifically, our tasks are to: (1) investigate the seasonal dynamics in stem radial increment under subtropical monsoon climate characterized by mild winters and hot summers; and (2) determine whether growth-limiting factor

switches from temperatures during spring and early summer to moisture variables during summer and autumn.

## 2. Materials and Methods

### 2.1. Study Site

This study was conducted in the Lushan Natural Reserve, in the north of Jiangxi Province, China. The study site was located at a permanent forest plot at the peak of the Lushan Mountains (29°33′39.8″ N, 115°59′14.6″ E, 1402 m a.s.l.). The forest plot is dominated by Taiwan pine with a stand basal area of 25.0 m<sup>2</sup> ha<sup>-1</sup> and a stand density of 925 trees ha<sup>-1</sup>. The regional climate is classified as subtropical monsoon climate, which is characterized by hot summers and mild winters. Long-term records (1980–2011) from the meteorological station in Lushan Mountains (29°35′ N, 115°59′ E, 1165 m a.s.l.) show that the annual mean temperature is 11.9 °C, with July as the hottest month (22.5 °C). The annual precipitation is 2009 mm, 58.2% of which is received during March to July (Figure 1). There is a dry season (July–November), influenced by the west Pacific subtropical high [14].

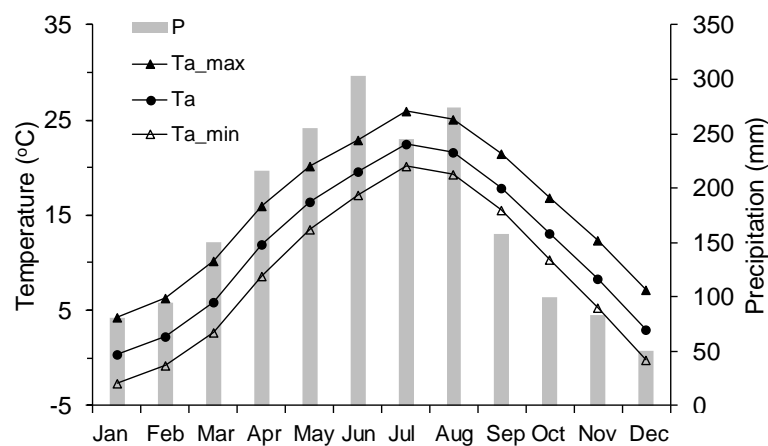


**Figure 1.** Monthly maximum (Ta\_max), mean (Ta), minimum (Ta\_min) temperatures and monthly precipitation (P) of Lushan from 1980 to 2011.

### 2.2. Dendrometer Measurements

In the forest plot, four mature and healthy Taiwan pine trees with similar dominance and age were selected to diminish the tree size effects on stem growth. The monitored trees had an average diameter at breast height (DBH) of 20.1 ± 2.4 cm, height of 5.9 ± 0.8 m, and tree age of 33 ± 4 year. Automatic band dendrometers equipped with built-in data loggers (DRL26C, EMS, Brno, Czech Republic) were used to continuously monitor stem radius variations. All dendrometers were mounted at breast height of each sampled tree. To reduce the influence of bark swelling and shrinkage and to ensure a close contact with stems, the outermost parts of the bark were carefully removed before installation. The measurement of stem circumference is achieved by attaching a stainless tape to the tree trunk and measuring displacements with a rotary position sensor. The dendrometer has an accuracy of 1 μm over a maximum range of 64 mm. Measurements were hourly collected by an internal data logger (DRL26C, EMS, Brno, Czech Republic) from March 2016 to November 2017. Due to technical problems, measurements of one monitored tree in 2016 were not available. Therefore, measurements of three and four sampled trees were used for further analyses in 2016 and 2017, respectively. All raw data were converted to stem radius variations assuming a circular stem of the sampled trees.

### 2.3. Environmental Data

Environmental data at the forest plot were simultaneously monitored with a 3-m high automated weather station (HOBO U30, Onset Corp., Bourne, MA, USA) since March 2016. A set of probes for measuring air temperature ( $T_a$ ; S-THB-M002, accuracy  $\pm 0.2$  °C) and relative humidity (RH; S-THB-M002, accuracy  $\pm 2.5\%$ ), precipitation (P; S-RGB-M002, resolution 0.2 mm), solar radiation (Ra; S-LIB-M003, accuracy  $\pm 10$  W m<sup>-2</sup>) and wind speed (W-WSB-M003, accuracy  $\pm 1.1$  m s<sup>-1</sup>) were mounted at a height of 3 m above the ground. Soil temperature ( $T_s$ ; S-TMB-M006, accuracy  $\pm 0.2$  °C) and volumetric soil moisture content (SM; S-SMD-M005, accuracy  $\pm 0.033$  m<sup>3</sup> m<sup>-3</sup>) were measured at 10 cm soil depth. Data were collected every 30 s and half-hour averages were stored in a data logger (U30-NRC, Onset Corp., Bourne, MA, USA). Vapor pressure deficit (VPD) was calculated from the half-hourly recorded air temperature and relative humidity [39]. To harmonize the time resolution between dendrometer measurements and environmental data, hourly averages or sums of environmental data were calculated.

### 2.4. Determination of Growing Season

It is recommended that examining the relationships between dendrometer-based stem increments and environmental variables should be performed during the stem growth period [25]. Since the raw data of a dendrometer are a combination of growth- and water-induced stem radius variations [25,40], appropriate algorithms are required for detecting the growing season from dendrometer data.

The Gompertz function is one of the most widely applied models to describe seasonal growth patterns due to its flexibility and asymmetrical shape [20,41]. Given the longer growing seasons in the subtropics [32], the year-round dendrometer data were used to determine the actual growing season of Taiwan pine. Using daily maximum values of dendrometer data during 2016–2017, the seasonal growth patterns across trees and observed years were identified by the Gompertz function as described by Duchesne et al. [41], in which the Gompertz model includes a parameter ( $y_0$ , the lower asymptote) indicative of the initial state at the beginning of growing season to avoid the arbitrary selection of initial settings of dendrometer data:

$$y = y_0 + a \times \exp[-\exp(\beta - \kappa \times t)] \quad (1)$$

where  $y$  is the daily maximum raw measurements;  $a$  is the upper asymptote;  $\beta$  is the  $x$ -axis placement parameter;  $\kappa$  is the rate of change parameter; and  $t$  is the time (expressed as day of year, DOY). The parameter estimation was performed with ordinary least squares method (SAS Institute, 2002) [30,41]. To evaluate the inter-tree variability, the seasonal growth patterns of individual trees ( $n = 3$ –4) for each year ( $n = 2$ ) were modeled. We also modeled the averaged stem radius variation for all trees in each year. In this study, the timing of growth initiation and cessation was estimated according to the dendrometer accuracy, though determinations of growth initiation and cessation from dendrometer data could be easily interfered with by stem swelling caused by rehydration in tree stems [40]. Specifically, the onset and ending dates of stem radial increment were defined as the DOY when modeled daily growth rates exceeded and fell below  $2 \mu\text{m day}^{-1}$ , respectively.

### 2.5. Extraction of Stem Radial Increment

Since the raw dendrometer measurements comprise irreversible stem growth and water-related reversible stem shrinking and swelling, several conceptual partitioning approaches have been proposed to extract the diurnal phases of stem radial variation [20,21,25]. In this study, stem cycle approach was used to disentangle different phases from time series of raw dendrometer measurements [19,20]. This approach divides the stem diurnal cycle into three distinct phases: (1) contraction, the period between the morning maximum radius and subsequent afternoon minimum; (2) recovery, the period from minimum to the position of the previous maximum value; and (3) radial increment, the period in which stem radius exceeds the morning maximum until the following maximum, which has

been considered as an estimate of actual stem growth (Figure 2). When the previous maximum was not exceeded, the radial increment phase was not determined and was treated as zero values (i.e., zero increment) in the subsequent analyses [20]. According to these definitions, the magnitude, duration and corresponding environmental variables of three phases for each stem diurnal cycle were individually computed for each tree in each year. To assess the general response of stem increments to environmental factors, stem-phase parameters were also calculated for averaged stem radius variation in each year. As we were interested in examining the growth-climate relationships, only radial-increment phase was used for further analyses. Analyses were performed using a specially developed R package (dendrometeR) by Van der Maaten et al. [42] using the R software (version 3.3.3, R Development Core Team, Vienna, Austria, 2015).

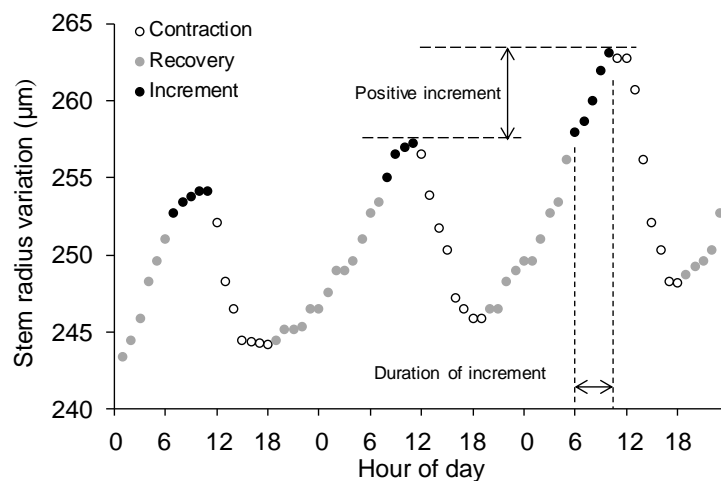


**Figure 2.** Schematic figure of the diurnal cycle of stem radius variation recorded by automatic dendrometer in Taiwan pine. The diurnal cycles are divided into three distinct phases: contraction, recovery and increment. The magnitude and duration of stem increment are indicated. Each circle represents an hourly measurement recorded in August 2017.

## 2.6. Data Analysis

To examine the temporal stability of growth-climate relationships for Taiwan pine throughout the growing seasons, moving correlation analysis was applied between stem increments and corresponding environmental variables. The moving correlation window was set to 21 days, which provided a robust association between stem increments and environmental variables. Since precipitation and soil moisture were non-normally distributed, nonparametric Spearman correlation coefficients were determined. Further, to investigate whether growth-limiting factors switch from temperatures during spring and early summer to moisture variables (precipitation and soil moisture) during summer and autumn, Spearman correlation coefficients were separately calculated in pre-early July (i.e., spring-early summer) and post-early July (i.e., summer-autumn) growing phases.

Differences in the monthly mean magnitude and duration of stem increment among growing-season months were analyzed by one-way ANOVA and the Tukey comparison (the Tukey–Kramer test is performed by SPSS software when group sizes are unequal).

All statistical analyses were conducted using the statistical package IBM SPSS 22.0 for Windows (SPSS Inc., Chicago, IL, USA), and all significant differences were taken at  $p < 0.05$ .

### 3. Results

#### 3.1. Environmental Conditions

During the main growing period (March–November), monthly mean air temperature ranged from 5.7 (March) to 21.0 °C (July) in 2016, and from 4.8 (March) to 21.3 °C (July) in 2017, respectively (Figure 3b,f). There was a comparable mean air temperature of 14.7 and 14.5 °C during March to November in 2016 and 2017. However, the mean air temperature during March to June in 2016 was 0.7 °C higher than that in 2017 (12.9 vs. 12.2 °C), and the mean air temperature during July to November was almost similar in two years (16.2 °C; Figure 3b,f). Maximum air temperature in both years reached 31.0 °C in late July. Soil temperature generally followed the seasonal trend of air temperature with less amplitudes (Figure 3b,f).

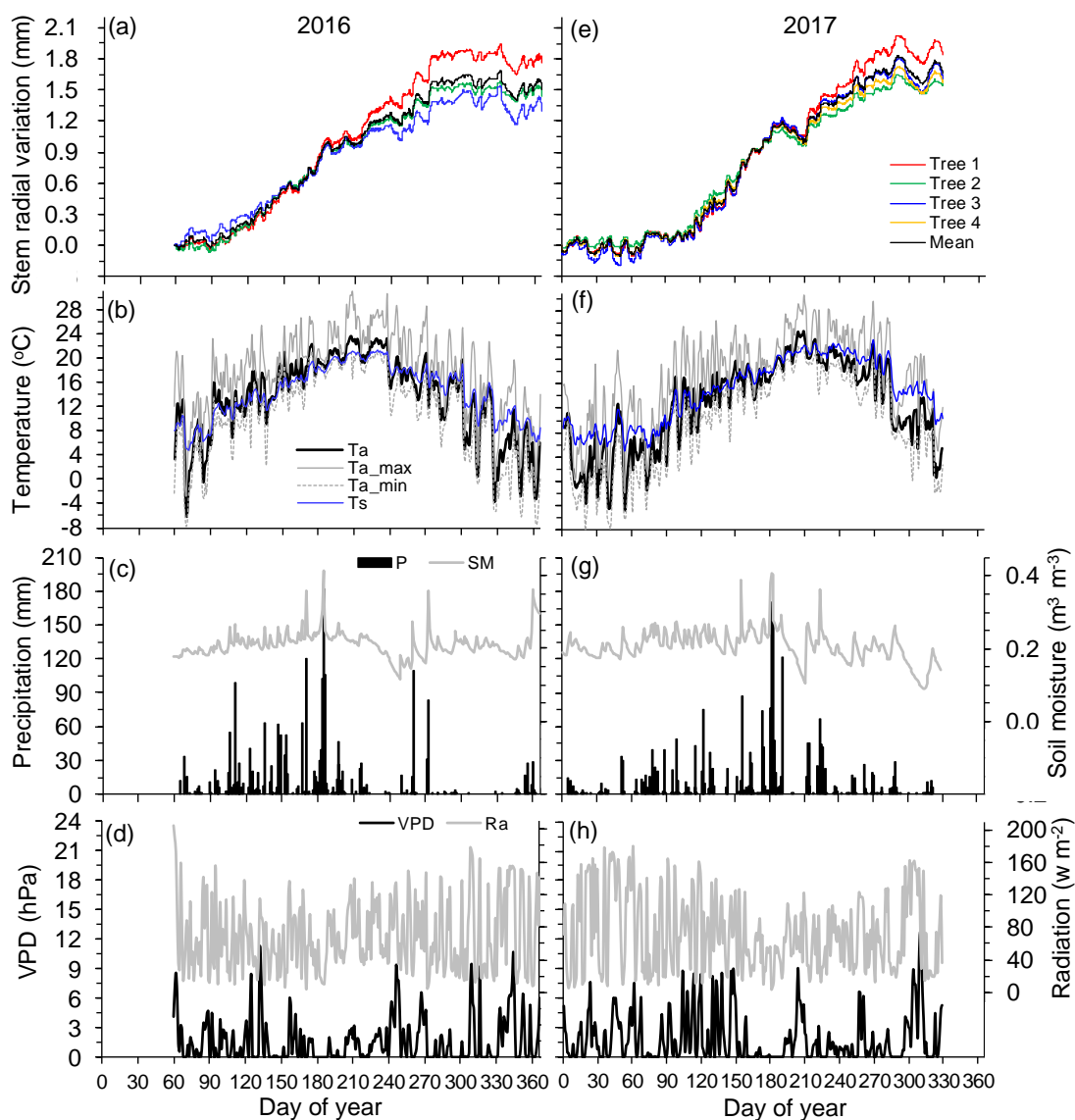


**Figure 3.** Annual courses of hourly radial records of monitored trees (a,e), air and soil temperatures (Ta, mean air temperature; Ta\_max, maximum air temperature; Ta\_min, minimum air temperature; Ts, mean soil temperature) (b,f), precipitation (P) and soil moisture (SM) (c,g), vapor pressure deficit (VPD) and solar radiation (Ra) (d,h) during 2016 and 2017.

From March to November, the sums of precipitation were 2104 mm in 2016 and 2165 mm in 2017, most of which (75.4% in 2016 and 73.3% in 2017) were recorded during March to early July (Figure 3c,g). In contrast, few precipitation events were observed since mid-July, which was more evident in 2016. In addition, the precipitation sum during July to November in 2017 was 161 mm higher than that in 2016 (Figure 3c,g). In late summers (mid-July to August), high temperatures combined with low rainfall caused a gradual decrease in soil moisture to a minimum of  $0.12 \text{ m}^3 \text{ m}^{-3}$  in September 2016 and  $0.11 \text{ m}^3 \text{ m}^{-3}$  in July 2017, respectively (Figure 3c,g). Vapor pressure deficit and solar radiation showed no obvious seasonal trends across years (Figure 3d,h).

### 3.2. Seasonal Growth Patterns and Dynamics of Stem Radial Increments

In both years, the seasonal pattern of stem radial variations was characterized by a progressive increase of stem radius in spring and early summer (mid-March to early July), followed by a plateau (2016) or marked decrease (2017) of stem radius in summer, and a sharp increase in late summer and autumn (August to October). The stem radial variation started to stabilize in November (Figure 3a,e). The pronounced winter shrinkage of stem radius was not observed during winter months because mean air temperature was generally above  $-4 \text{ }^\circ\text{C}$  with occasional occurrence of  $<0 \text{ }^\circ\text{C}$  in maximum air temperature [24] (Figure 3).

Gompertz models explained between 98% and 99% of the variation in daily maximum stem radius data (Figure 4a,c). On average, stem growth synchronously started around 21 March in 2016 (DOY  $81 \pm 7$ ) and 7 days earlier in 2017 (DOY  $74 \pm 4$ ). However, the cessation of stem growth ranged from 18 October to 27 November (DOY 292–332) in 2016, and from 17 October to 30 November (DOY 290–334) in 2017 (Table 1, Figure 4b,d). Consequently, the average duration of growing season was 229 and 233 days in 2016 and 2017, respectively. The averaged cumulative seasonal growth of studied trees (Tree 1–3) was  $1.65 \pm 0.32$  and  $1.84 \pm 0.27$  mm in 2016 and 2017, respectively (Table 1).

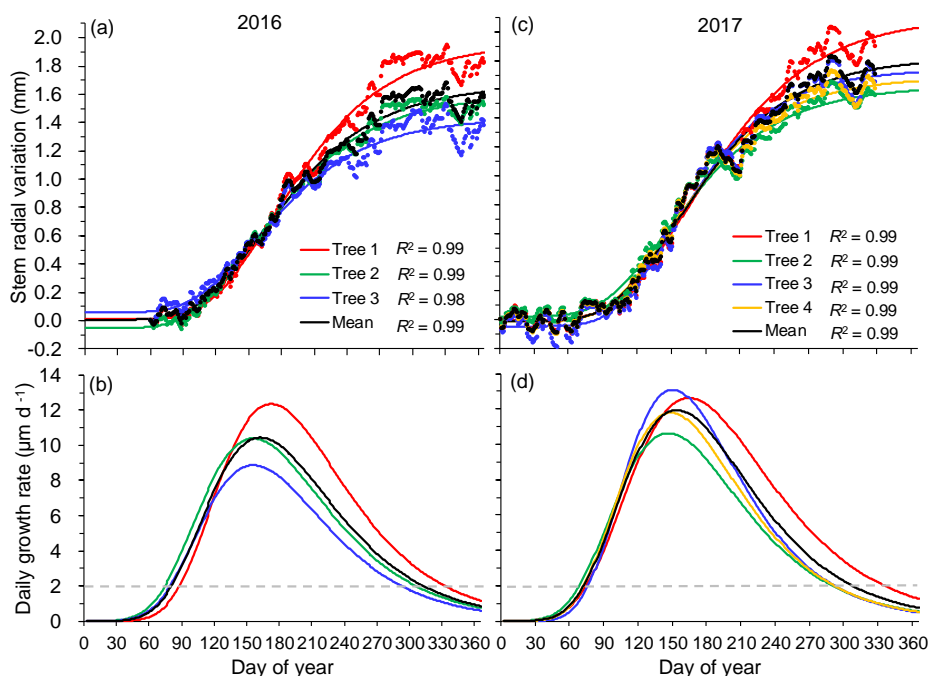


**Figure 4.** Observed and modeled stem radial variations (a,c) and associated daily growth rate (b,d) of Taiwan pine in 2016 and 2017. Dots and lines in top panels represent raw measurements of daily maximum radius and Gompertz function modeled curves, respectively. Dashed lines in the bottom panels indicate daily growth rates equal to  $2 \text{ } \mu\text{m day}^{-1}$ , which correspond to the dendrometer accuracy.

**Table 1.** Timing of growth onset and ending, and cumulative seasonal growth in 2016 and 2017. Onset and end of stem radial growth were estimated from the Gompertz function and given as day of year (DOY).

Year	Trees	Onset of Growth (DOY)	Ending of Growth (DOY)	Growing Season Length (Days)	Cumulative Seasonal Growth (mm)
2016	Tree 1	89	332	244	1.94
	Tree 2	75	305	231	1.70
	Tree 3	80	292	213	1.32
	Mean	81	312	232	1.65
2017	Tree 1	75	334	260	2.12
	Tree 2	69	290	222	1.58
	Tree 3	77	292	216	1.83
	Tree 4	73	291	219	1.71
	Mean	73	307	235	1.84

In both years, individual trees showed the same daily stem increment variation pattern throughout the two growing seasons, in which zero increments occurred frequently after early July, but a few days with high stem increments were also present (Figure 5). On a monthly basis, stem increments ranged from 0.01 to 0.09 mm over the two growing seasons, with a bimodal pattern in 2016 and less pronounced in 2017 (Figure 6a). From March to June, stem increments progressively increased until reaching a peak in early summer (May–June) ( $p < 0.05$ ). However, stem increments were significantly decreased during summer periods (July–August) in both years ( $p < 0.05$ ). In autumn, precipitation events promoted another peak of stem increment in September 2016 ( $p < 0.05$ ) and in October 2017. Similar seasonal dynamics were also found in the duration of stem increments, in which the average durations of stem increments were 7.9 h (7.8 h in 2016 and 8.1 h in 2017) during April–June and 6.4 h (6.7 h in 2016 and 6.2 h in 2017) during September–October, whereas the durations of stem increments were significantly decreased during July–August (4.2 h for both years,  $p < 0.05$ ) (Figure 6b). Also, there was a robust positive correlation between amplitude and duration of stem increments ( $r = 0.77–0.82$ ,  $p < 0.05$ ; data not shown).

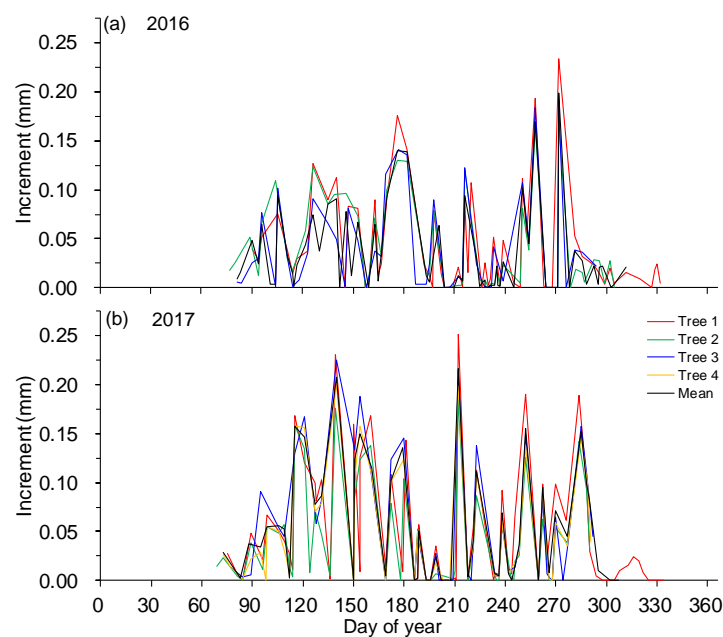


**Figure 5.** Time series of stem increments of four trees extracted for the growing periods of (a) 2016 and (b) 2017.

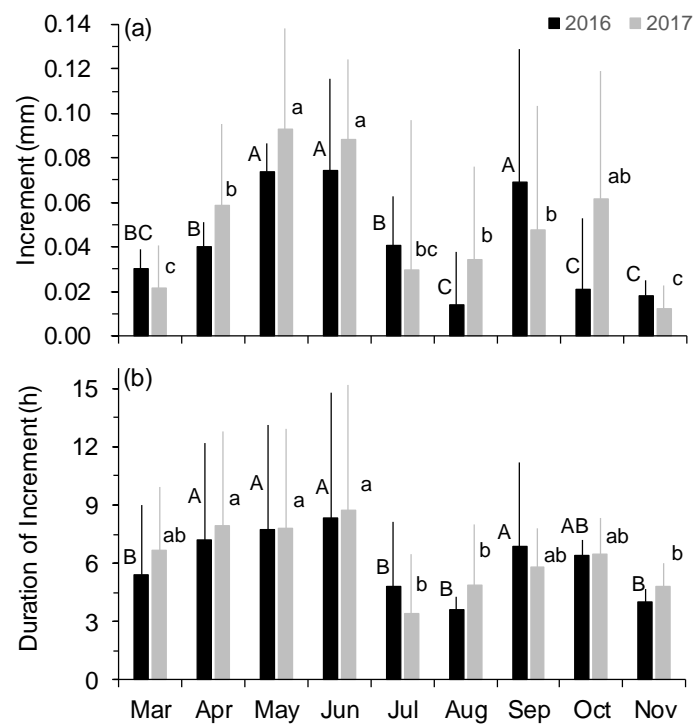


**Figure 6.** Variations of monthly mean magnitude (a) and duration (b) of stem increment during the two growing seasons. Different letters indicate significant difference in magnitude and duration of stem increment among months in 2016 (uppercase) and 2017 (lowercase) at  $p < 0.05$ . Error bars indicate  $\pm$  SD of mean.

### 3.3. Correlations of Stem Increments to Environmental Factors

Taking the whole growing season into account, stem increments showed the closest correlation with minimum air temperature (negative relationship) in 2016, while a significant positive relationship was found between stem increments and precipitation in 2017 (Table 2). As expected, moving correlation analysis consistently indicated a strong shift in growth-limiting factors around DOY 185 in both years (Figure 7). Stem increments for both years showed significant positive correlations with mean and maximum air temperatures ( $p < 0.05$ ) before early July (i.e., DOY 185), whereas the correlations between stem increment and temperatures dramatically decreased to insignificance ( $p > 0.05$ ) after early July. In general, similar temporal variations in growth-climate relationships were also found between stem increments and soil and minimum air temperatures (Supplementary Figure S1). In contrast, the opposite trend of insignificant and robust correlations between stem increments and moisture variables of precipitation and soil moisture was observed before and after early July, respectively. However, stem increments varied little with vapor pressure deficit and solar radiation throughout the two growing seasons (data not shown). Therefore, the growing seasons were divided into two phases (i.e., pre- and post-early July), and consistent results were obtained between years (Table 2). Stem increments in pre-early July were mainly limited by mean and maximum air temperatures, whereas moisture variables mainly determined the variations of stem increments in post-early July, and high temperatures also had a suppressing effect on stem growth.

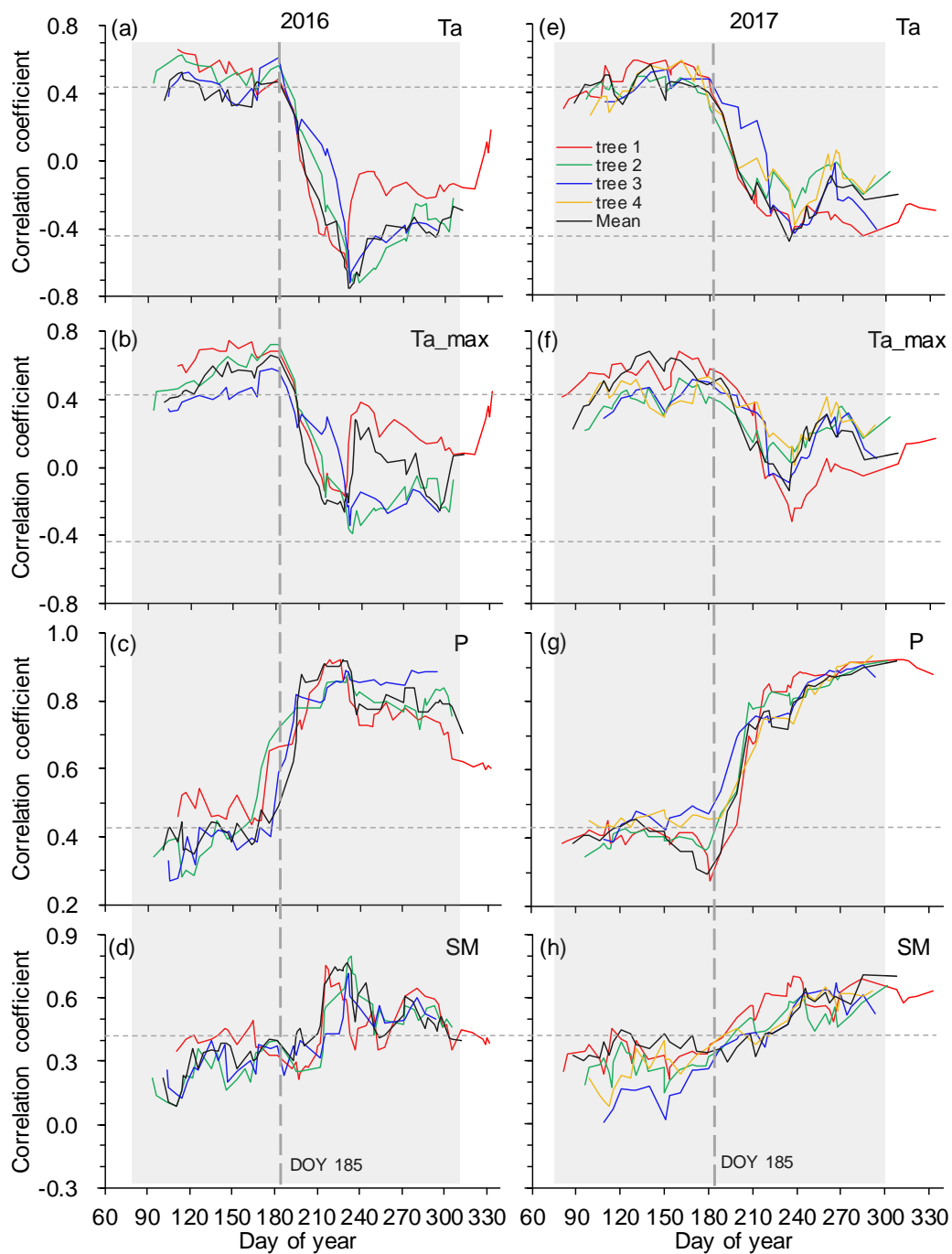


**Figure 7.** Moving correlations (21 days window) between stem increments and environmental variables of mean air temperature (**a,e**), maximum air temperature (**b,f**), precipitation (**c,g**), and soil moisture (**d,h**) during the growing seasons in 2016 and 2017. Spearman correlations were calculated for relationships between stem increments and all environmental variables. Horizontal thin dashed lines indicate the significance level at  $p = 0.05$ . Vertical thick dashed lines indicate the timing of shifts in the correlations between stem increments and environmental variables. The shaded regions indicate the growing seasons.

**Table 2.** Spearman correlation coefficients between stem increments and environmental variables (mean air temperature (Ta, °C), maximum air temperature (Ta\_max, °C), minimum air temperature (Ta\_min, °C), mean soil temperature (Ts, °C), precipitation (P, mm), soil moisture (SM, m<sup>3</sup> m<sup>-3</sup>), vapor pressure deficit (VPD, hPa), and solar radiation (Ra, W m<sup>-2</sup>)) during the whole growing season and two separated growing phases in 2016 and 2017. Pre- and post-early July growing phases were separated by DOY 185 (see Figure 7).

Independent Variables	2016			2017		
	Whole Growing Season	Pre-Early July	Post-Early July	Whole Growing Season	Pre-Early July	Post-Early July
Ta	−0.25 *	0.51 **	−0.41 *	−0.17	0.68 **	−0.26
Ta_max	−0.07	0.64 ***	−0.05	0.15	0.61 **	0.09
Ta_min	−0.37 **	0.28	−0.50 **	−0.29 *	0.24	−0.44 *
Ts	−0.22	0.50 **	−0.25	−0.15	0.51 *	−0.13
P	0.34 **	0.39	0.76 ***	0.65 ***	0.44	0.88 ***
SM	0.24	0.31	0.52 **	0.51 ***	0.39	0.59 **
VPD	−0.16	−0.03	−0.19	−0.05	−0.10	−0.28
Ra	−0.06	−0.26	0.08	−0.04	−0.05	−0.07

\*  $p < 0.05$ , \*\*  $p < 0.01$ , \*\*\*  $p < 0.001$ .

## 4. Discussion

### 4.1. Seasonal Dynamics of Stem Radial Growth

In subtropical climates, the dynamic of stem radial growth is limited by the double climatic stress of the mild winters and hot summers [43,44]. In this study, the stem radial growth of Taiwan pine started around mid-March in both years, but the ending date ranged from mid-October to late November. Moreover, the bimodal stem radial growth pattern with two growth peaks in transitional seasons (spring-early summer and autumn) and a decreased growth rate in summer was detected, though it was less evident in 2017. The bimodal seasonal growth pattern is in accordance with a recent intra-annual xylem growth observation of Masson pine (*Pinus massoniana* Lamb.) in subtropical China [32]. In the Mediterranean areas, seasonal dynamics of radial-increment revealed a similar capacity of several conifer species to resume cambial activity after a period of minimum growth or dormancy during summer droughts [45–47]. The summer growth suppression seems to be a strategy for coping with harsh environmental conditions during the summer drought. Under high temperatures and little rainfall, strong transpiration amplified the magnitude and duration of daytime contraction within tree stems, and refilling its hydraulic capacitance was restricted due to low soil water availability [48], thus resulting in the shrinkage of the stems and decreased magnitude and duration of stem increments of Taiwan pine. However, autumn rainfall could reactivate cambial activity, which might have led to the second peak of stem increments in autumn [45–47]. The less clear autumn growth peak in 2017 was probably related to early sporadic late-summer rainfall events, suggesting a high plasticity of seasonal dynamics of radial-increment in response to varying intensity and duration of summer droughts.

Temperature has been considered to play an important role in controlling onset of stem growth in spring across temperate and boreal forests [49–51]. It has been demonstrated that xylem cell production of conifers in cold environments often reactivates when a critical mean daily air temperature of 4–5 °C is reached [49]. In this study, mean air temperatures during the 10-day period before the onset of stem growth were 4.8 °C in 2016 and 4.1 °C in 2017, and mean soil temperatures were 6.8 °C in 2016 and 8.3 °C in 2017. The one-week earlier onset of stem growth of Taiwan pine in 2017 compared to 2016 might be attributed to the difference in soil temperature between years. Such a stimulating effect of soil temperature on initiation of stem growth was also found at mountain forest plots with open sparse canopy [52]. Although soil water is available in early spring, low soil temperatures can not only hamper root growth but also restrict root water uptake and above-ground transpiration [53],

which in turn affects the cell turgor and enlargement of newly-produced xylem cells in the stem. However, there is evidence that low soil temperature no longer affects tree transpiration when it rises to ca. 8 °C [53,54]. Thus, our data suggests that the relatively low soil temperature in early spring may induce water deficit in tree stems, resulting in a later growth initiation. In contrast, the timing of stem growth cessation varied considerably among tree individuals and between two years. Similar results were also found in conifers across mountain and boreal forests [30,41,50,55]. This variation indicates that temperature variables have a minor influence in determining the ending of growth, while it is probably regulated by complex endogenous physiological mechanisms [41].

#### 4.2. Seasonal Shift in Growth–Climate Relationships

In southeast China, the climate is characterized by the Eastern-Asian monsoon with mild winters and hot summers. This double seasonal climatic stress clearly implies that climatic conditions in spring and summer–autumn may have contrasting effects on tree growth. However, previous dendroclimatic investigations have indicated intricate relationships between tree growth and climate in this region [13–16,36,37,56]. Mechanisms of how seasonal tree growth responds to such climate seasonality are critical to understand the limitations to tree growth. In this study, on intra-annual time resolution, changing growth–climate relationships between stem increments and temperature and moisture variables were found over the two growing seasons, which induced the switching of growth-limiting factor from temperatures in spring and early summer to precipitation in summer and autumn. This seasonal shift in growth-limiting factors has been broadly observed across coniferous and deciduous tree species in temperate forests under summer drought [27,34,57].

In temperate and cold-limited forests, stem radial growth is generally thought to be limited by temperature [20,58,59], particularly at the beginning and end of growing seasons [34]. However, contrasting effects of temperature on stem radial increment may occur in different growing phases, which is possibly associated with an optimum temperature [7,34,57]. Physiologically, the stimulating effects of temperature on stem radial growth involve allocating photosynthates to the process of cambium activity and xylem formation and allowing the metabolic process of growth to be completed [49,60,61]. At the cellular level, it has been observed that cambial cell division mainly occurs in the early part of growing season when temperature is favourable for growth, in which cell production rate consistently shows a positive response to temperature [40,62,63]. However, temperatures above a certain threshold (ranging from 16 to 21 °C for conifers [57,64,65]) can induce a reduction in net photosynthesis due to increased photorespiration [66,67], which in turn results in a negative effect on stem radial growth. For Taiwan pine, the timings of rapid decrease in the moving correlations between temperatures and stem increments roughly corresponded to a mean air temperature of 19–20 °C, which well matched with the thermal optimum for photosynthesis [35], suggesting that summer temperatures exceeded the optimum.

In post-early July, high temperatures were unfavorable for leaf stomata conductance and could also enhance respiration rates [48,55,61], both of which decreased the available carbohydrates for stem radial growth, resulting in the negative correlations between stem increments and temperatures. Conversely, during this dry period, large amounts of precipitation (>15 mm day<sup>-1</sup>) indirectly alleviated water deficit in tree stems through sharply increasing soil moisture, which caused less negative water potentials that favor cell enlargement [28,29,68,69]. On the other hand, light rain events (<15 mm day<sup>-1</sup>) directly induced a partial release of the low needle water potential through wetting the crown, leading to an increase in cambial turgor and thus to an enlargement of the existing xylem cells [28,69]. Consequently, the effects of moisture variables on stem increments overwhelm that of temperatures in post-early July. Such mechanisms well explain why the growth-limiting factor switched from temperatures in spring and early summer to precipitation in summer and autumn.

Temperatures as the growth-limiting factor during spring and early summer confirms the results from dendroclimatological studies of Taiwan pine in southeast China, in which radial growth was positively correlated to temperatures during February–July [13,15,36,70,71]. Also, the early-season

temperature constraint on tree-ring width was reported for other conifers in subtropical China [72]. Nevertheless, non-significant relationships between precipitation and tree-ring width were obtained in these dendroclimatic studies. This result contrasts with our finding that moisture variables (precipitation and soil moisture) played an important role in determining stem increments during summer and autumn. The fading impact of summer-autumn precipitation on tree-ring width is probably due to the fact that up to 67% of the total width was already produced before early July (data not shown), suggesting that summer-autumn precipitation signals revealed by tree-ring width may mix with the climate signals of other seasons. However, at low-elevation sites in southeast China where a large part of ring width was mainly formed in September (i.e., during drought periods), tree growth of Masson pine was limited by summer and autumn precipitation [73]. Further evidence of a seasonal shift in growth-limiting factors is that ring width of Masson pine from mid-elevation sites was concurrently and positively correlated with early-season temperature and summer-autumn precipitation [74]. Moreover, our findings imply that different intra-ring sector widths (i.e., earlywood and latewood) rather than total ring widths may reflect detailed seasonal climate information. Indeed, the latewood width of *Tsuga longibracteata* Cheng did represent a reliable proxy for summer-autumn precipitation in south China [75].

Studies on wood formation have documented that tree-ring width is highly sensitive to changes in seasonality of growing-season climate [34]. In this study, despite the almost similar growing-season temperature and precipitation (averages or sums during March–November) between the two study years, a wider annual increment in 2017 compared to 2016 was observed. Since stem increments in different seasonal growing phases were separately limited by contrasting climatic factors, differences in annual increment between the two years were attributed to the intra-annual variations in climatic conditions. Although tree growth started earlier in 2017 than that in 2016, trees did not produce much more cumulative stem increments until early July (data not shown), which was mainly associated with the lower spring-early summer temperature in 2017 [76]. During the dry period (July–November), however, the year 2017 received more precipitation than 2016, which greatly promoted the stem radial growth. While the effect of spring-early summer temperature on ring width may depend on the balance between the timing of growth initiation and growth rate, our results highlight the important constraint of summer drought on ring width in subtropical China. In fact, there is evidence that increased intensity of summer drought in recent decades in south China had induced a decadal change in growth-limiting factors of *Fokienia hodginsii* (Dunn) Henry et Thomas from January–April mean temperature to August–September precipitation [77]. In the future, detailed investigations of xylogenesis in histological sections and long-term tree-ring widths as well as intra-ring sector widths are needed to further elucidate the mechanisms of how tree growth of Taiwan pine responds to changing environmental constraints in subtropical China.

## 5. Conclusions

Stem radius variations of montane Taiwan pine in southeast China were monitored with high-resolution band dendrometers over a two-year period. Our data revealed a bimodal seasonal pattern of stem radial increments though it was less evident in 2017, indicating that radial growth was limited by the double climatic stress of mild winters and hot summers under the Eastern-Asian monsoon climate. On intra-annual time resolution, the growth-limiting factor switched from temperatures in spring and early summer to precipitation in summer and autumn, which was probably related to the excess of temperature over an optimum threshold and drought stress during the mid to late growing season. This study provides a fundamental understanding of the role of temperature and precipitation in controlling intra-annual stem radial growth in subtropical forests, and highlights the importance of identifying seasonal shifts in growth-limiting factors in forecasting growth responses to climate change in south China. Given that the climate in south China is getting warmer and drier due to the increased frequency and intensity of summer drought [10,73,77], our results suggest that annual increments do not necessarily increase, as the promotion effect of warm temperature on

growth initiation and growth rate in the first part of the growing season may be offset by the negative consequences of drought on growth in the second part of the growing season.

**Supplementary Materials:** The following are available online at <http://www.mdpi.com/1999-4907/9/7/387/s1>, Figure S1: Moving correlations (21 days window) between stem increments and minimum air (a,c) and soil (b,d) temperatures during the growing seasons in 2016 and 2017. Spearman correlations were calculated for relationships between stem increments and temperature variables. Horizontal thin dashed lines indicate the significance level at  $p = 0.05$ . Vertical thick dashed lines indicate the timing of shifts in the correlations between stem increments and temperature variables. The shaded regions indicate the growing seasons.

**Author Contributions:** X.L. conceived and designed the experiments. X.L., Y.N. and F.W. performed the experiments. X.L. and Y.N. analyzed the data and wrote the paper. F.W. reviewed and edited the draft.

**Funding:** This work was supported by the National Natural Science Foundation of China (grant No. 41561011), and the Natural Science Foundation of Jiangxi, China (grant No. 20151BAB213029).

**Acknowledgments:** We thank S.Y. Wu and L.L. Cai for their help in the field investigation.

**Conflicts of Interest:** The authors declare no conflict of interest.

## References

1. Prentice, I.C.; Heimann, M.; Sitch, S. The carbon balance of the terrestrial biosphere: Ecosystem models and atmospheric observations. *Ecol. Appl.* **2000**, *10*, 1553–1573. [[CrossRef](#)]
2. Cuny, H.E.; Rathgeber, C.B.K.; Frank, D.; Fonti, P.; Mäkinen, H.; Prislan, P.; Rossi, S.; del Castillo, E.M.; Campelo, F.; Vavřík, H.; et al. Woody biomass production lags stem-girth increase by over one month in coniferous forests. *Nat. Plants* **2015**, *1*, 15160. [[CrossRef](#)] [[PubMed](#)]
3. Tardif, J.; Camarero, J.J.; Ribas, M.; Gutiérrez, E. Spatiotemporal variability in tree growth in the Central Pyrenees: Climatic and site influences. *Ecol. Monogr.* **2003**, *73*, 241–257. [[CrossRef](#)]
4. Boisvenue, C.É.L.; Running, S.W. Impacts of climate change on natural forest productivity—evidence since the middle of the 20th century. *Glob. Chang. Biol.* **2006**, *12*, 862–882. [[CrossRef](#)]
5. Briffa, K.R.; Bartholin, T.S.; Eckstein, D.; Jones, P.D.; Karlén, W.; Schweinguber, F.H.; Zetterberg, P. A 1400-year tree-ring record of summer temperatures in Fennoscandia. *Nature* **1990**, *346*, 434–439. [[CrossRef](#)]
6. Esper, J.; Cook, E.R.; Schweingruber, F.H. Low frequency signals in long tree-ring chronologies for reconstructing past temperature variability. *Science* **2002**, *295*, 2250–2253. [[CrossRef](#)] [[PubMed](#)]
7. Wilmking, M.; Juday, G.P.; Barber, V.A.; Zald, H.S.J. Recent climate warming forces contrasting growth responses of white spruce at treeline in Alaska through temperature thresholds. *Glob. Chang. Biol.* **2004**, *10*, 1724–1736. [[CrossRef](#)]
8. Liu, H.; Williams, A.P.; Allen, C.; Guo, D.; Wu, X.; Anenkhonov, O.A.; Liang, E.Y.; Sandanov, D.; Yin, Y.; Qi, Z.; et al. Rapid warming accelerates tree growth decline in semi-arid forests of Inner Asia. *Glob. Chang. Biol.* **2013**, *19*, 2500–2510. [[CrossRef](#)] [[PubMed](#)]
9. Yu, G.; Chen, Z.; Piao, S.; Peng, C.; Ciais, P.; Wang, Q.; Li, X.; Zhu, X. High carbon dioxide uptake by subtropical forest ecosystems in the East Asian monsoon region. *Proc. Natl. Acad. Sci. USA* **2014**, *111*, 4910–4915. [[CrossRef](#)] [[PubMed](#)]
10. Zhou, G.; Wei, X.; Wu, Y.; Liu, S.; Huang, Y.; Yan, J.; Zhang, D.; Zhang, Q.; Liu, J.; Meng, Z.; et al. Quantifying the hydrological responses to climate change in an intact forested small watershed in Southern China. *Glob. Chang. Biol.* **2011**, *17*, 3736–3746. [[CrossRef](#)]
11. Liang, E.Y.; Shao, X.M.; Xu, Y. Tree-ring evidence of recent abnormal warming on the southeast Tibetan Plateau. *Theor. Appl. Climatol.* **2009**, *98*, 9–18. [[CrossRef](#)]
12. Dulamsuren, C.; Hauck, M.; Leuschner, C. Recent drought stress leads to growth reductions in *Larix sibirica* in the western Khentey, Mongolia. *Glob. Chang. Biol.* **2010**, *16*, 1960–2002. [[CrossRef](#)]
13. Shi, J.; Cook, E.R.; Lu, H.; Li, J.; Wright, W.E.; Li, S. Tree-ring based winter temperature reconstruction for the lower reaches of the Yangtze River in southeast China. *Clim. Res.* **2010**, *41*, 169–175. [[CrossRef](#)]
14. Chen, F.; Yuan, Y.J.; Wei, W.S.; Yu, S.L.; Zhang, T.W. Reconstructed temperature for Yong'an, Fujian, Southeast China: Linkages to the Pacific Ocean climate variability. *Glob. Planet. Chang.* **2012**, *86–87*, 11–19. [[CrossRef](#)]
15. Duan, J.P.; Zhang, Q.B.; Lv, L.X. Increased variability in cold-season temperature since the 1930s in subtropical China. *J. Clim.* **2013**, *26*, 4749–4757. [[CrossRef](#)]

16. Luo, D.; Huang, J.G.; Jiang, X.; Ma, Q.; Liang, H.; Guo, X.; Zhang, S. Effects of climate and competition on radial growth of *Pinus massoniana* and *Schima superba* in China's subtropical monsoon mixed forest. *Dendrochronologia* **2017**, *46*, 24–34. [[CrossRef](#)]
17. D'Arrigo, R.D.; Barbetti, M.; Watanasak, M.; Buckley, B.; Krusic, P.; Boonchirdchoo, S.; Sarutanon, S. Progress in dendroclimatic studies of mountain pine in northern Thailand. *IAWA J.* **1997**, *18*, 433–444. [[CrossRef](#)]
18. Fritts, H.C. *Tree Rings and Climate*; Academic Press: London, UK; New York, NY, USA; San Francisco, CA, USA, 1976.
19. Downes, G.; Beadle, C.; Worledge, D. Daily stem growth patterns in irrigated *Eucalyptus globulus* and *E. nitens* in relation to climate. *Trees* **1999**, *14*, 102–111. [[CrossRef](#)]
20. Deslauriers, A.; Morin, H.; Urbinati, C.; Carrer, M. Daily weather response of balsam fir (*Abies balsamea* (L.) Mill.) stem radius increment from dendrometer analysis in the boreal forests of Québec (Canada). *Trees Struct. Funct.* **2003**, *17*, 477–484. [[CrossRef](#)]
21. Zweifel, R.; Haeni, M.; Buchmann, N.; Eugster, W. Are trees able to grow in periods of stem shrinkage? *New Phytol.* **2016**, *211*, 839–849. [[CrossRef](#)] [[PubMed](#)]
22. Mencuccini, M.; Salmon, Y.; Mitchell, P.; Hölttä, T.; Choat, B.; Meir, P.; O'Grady, A.; Tissue, D.; Zweifel, R.; Sevanto, S.; et al. An empirical method that separates irreversible stem radial growth from bark water content changes in trees: Theory and case studies. *Plant Cell Environ.* **2017**, *40*, 290–303. [[CrossRef](#)] [[PubMed](#)]
23. Mencuccini, M.; Hölttä, T.; Sevanto, S.; Nikinmaa, E. Concurrent measurements of change in the bark and xylem diameters of trees reveal a phloem-generated turgor signal. *New Phytol.* **2013**, *198*, 1143–1154. [[CrossRef](#)] [[PubMed](#)]
24. King, G.; Fonti, P.; Nievergelt, D.; Büntgen, U.; Frank, D. Climatic drivers of hourly to yearly tree radius variations along a 6 °C natural warming gradient. *Agric. For. Meteorol.* **2013**, *168*, 36–46. [[CrossRef](#)]
25. Deslauriers, A.; Rossi, S.; Anfodillo, T. Dendrometer and intra-annual tree growth: What kind of information can be inferred? *Dendrochronologia* **2007**, *25*, 113–124. [[CrossRef](#)]
26. Köcher, P.; Horna, V.; Leuschner, C. Environmental control of daily stem growth patterns in five temperate broad-leaved tree species. *Tree Physiol.* **2012**, *32*, 1021–1032. [[CrossRef](#)] [[PubMed](#)]
27. Van der Maaten, E.; Bouriaud, O.; Van der Maaten-Theunissen, M.; Mayer, H.; Spiecker, H. Meteorological forcing of day-to-day stem radius variations of beech is highly synchronic on opposing aspects of a valley. *Agric. For. Meteorol.* **2013**, *181*, 85–93. [[CrossRef](#)]
28. Jiang, Y.; Wang, B.Q.; Dong, M.Y.; Huang, Y.M.; Wang, M.C.; Wang, B. Response of daily stem radial growth of *Platycladus orientalis* to environmental factors in a semi-arid area of North China. *Trees* **2015**, *29*, 87–96. [[CrossRef](#)]
29. Urrutia-Jalabert, R.; Rossi, S.; Deslauriers, A.; Malhi, Y.; Lara, A. Environmental correlates of stem radius change in the endangered *Fitzroya cupressoides* forests of southern Chile. *Agric. For. Meteorol.* **2015**, *200*, 209–221. [[CrossRef](#)]
30. Wang, Z.Y.; Yang, B.; Deslauriers, A.; Bräuning, A. Intra-annual stem radial increment response of Qilian juniper to temperature and precipitation along an altitudinal gradient in northwestern China. *Trees* **2015**, *29*, 25–34. [[CrossRef](#)]
31. Hu, L.; Fan, Z. Stem radial growth in response to microclimate in an Asian tropical dry karst forest. *Acta Ecol. Sin.* **2016**, *36*, 401–409. [[CrossRef](#)]
32. Zhang, S.; Huang, J.; Rossi, S.; Ma, Q.; Yu, B.; Zhai, L.; Luo, D.; Guo, X.; Fu, S.; Zhang, W. Intra-annual dynamics of xylem growth in *Pinus massoniana* submitted to an experimental nitrogen addition in Central China. *Tree Physiol.* **2017**, *37*, 1546–1553. [[CrossRef](#)] [[PubMed](#)]
33. Oberhuber, W.; Gruber, A. Climatic influences on intra-annual stem radial increment of *Pinus sylvestris* (L.) exposed to drought. *Trees* **2010**, *24*, 887–898. [[CrossRef](#)] [[PubMed](#)]
34. Oladi, R.; Elzami, E.; Pourtahmasi, K.; Bräuning, A. Weather factors controlling growth of Oriental beech are on the turn over the growing season. *Eur. J. For. Res.* **2017**, *136*, 345–356. [[CrossRef](#)]
35. Weng, J.H.; Lai, K.M.; Liao, T.S.; Hwang, M.Y.; Chen, Y.N. Relationships of photosynthetic capacity to PSII efficiency and to photochemical reflectance index of *Pinus taiwanensis* through different seasons at high and low elevations of sub-tropical Taiwan. *Trees* **2009**, *23*, 347–356. [[CrossRef](#)]
36. Zheng, Y.; Zhang, Y.; Shao, X. Temperature variability inferred from tree-ring widths in the Dabie Mountains of subtropical central China. *Trees* **2012**, *26*, 1887–1894. [[CrossRef](#)]

37. Shi, J.; Cook, E.R.; Li, J.; Lu, H. Unprecedented January–July warming recorded in a 178-year tree-ring width chronology in the Dabie Mountains, southeastern China. *Palaeogeogr. Palaeoclimatol. Palaeoecol.* **2013**, *381*–382, 92–97. [[CrossRef](#)]
38. Cai, Q.F.; Liu, Y. Two centuries temperature variations over subtropical southeast China inferred from *Pinus taiwanensis* Hayata tree-ring width. *Clim. Dyn.* **2017**, *48*, 1813–1825. [[CrossRef](#)]
39. Jones, H.G. *Plants and Microclimate: A Quantitative Approach to Environmental Plant Physiology*; Cambridge University Press: Cambridge, UK, 1983.
40. Mäkinen, H.; Nöjd, P.; Saranpää, P. Seasonal changes in stem radius and production of new tracheids in Norway spruce. *Tree Physiol.* **2003**, *23*, 959–968. [[CrossRef](#)] [[PubMed](#)]
41. Duchesne, L.; Houle, D.; D’Orangeville, L. Influence of climate on seasonal patterns of stem increment of balsam fir in a boreal forest of Québec, Canada. *Agric. For. Meteorol.* **2012**, *162*–163, 108–114. [[CrossRef](#)]
42. Van der Maaten, E.; Van der Maaten-Theunissen, M.; Smilianić, M.; Rossi, S.; Simard, S.; Wilmking, M.; Deslauriers, A.; Fonti, P.; von Arx, G.; Bouriaud, O. dendrometerR: Analyzing the pulse of trees in R. *Dendrochronologia* **2016**, *40*, 12–16. [[CrossRef](#)]
43. Krepkowski, J.; Bräuning, A.; Gebrekirstos, A.; Strobl, S. Cambial growth dynamics and climatic control of different tree life forms in tropical mountain forest in Ethiopia. *Trees* **2011**, *25*, 59–70. [[CrossRef](#)]
44. Deslauriers, A.; Fonti, P.; Rossi, S.; Rathgeber, C.B.K.; Gričar, J. Ecophysiology and Plasticity of Wood and Phloem Formation. In *Dendroecology: Tree-Ring Analyses Applied to Ecological Studies*; Amoroso, M.M., Daniels, L.D., Baker, P.J., Camarero, J.J., Eds.; Springer: Cham, Switzerland, 2017; pp. 13–33.
45. De Luis, M.; Gričar, J.; Čufar, K.; Raventós, J. Seasonal dynamics of wood formation in *Pinus halepensis* from dry and semi-arid ecosystems in Spain. *IAWA J.* **2007**, *28*, 389–404. [[CrossRef](#)]
46. Camarero, J.J.; Olano, J.M.; Parras, A. Plastic bimodal xylogenesis in conifers from continental Mediterranean climates. *New Phytol.* **2010**, *185*, 471–480. [[CrossRef](#)] [[PubMed](#)]
47. Vieira, J.; Campelo, F.; Rossi, S.; Carvalho, A.; Freitas, H.; Nabais, C. Adjustment Capacity of Maritime Pine Cambial Activity in Drought-Prone Environments. *PLoS ONE* **2015**, *10*, e0126223. [[CrossRef](#)] [[PubMed](#)]
48. Vieira, J.; Rossi, S.; Campelo, F.; Freitas, H.; Nabais, C. Seasonal and daily cycles of stem radial variation of *Pinus pinaster* in a drought-prone environment. *Agric. For. Meteorol.* **2013**, *180*, 173–181. [[CrossRef](#)]
49. Rossi, S.; Deslauriers, A.; Gričar, J.; Seo, J.-W.; Rathgeber, C.; Anfodillo, T.; Morin, H.; Levanic, T.; Oven, P.; Jalkanen, R. Critical temperatures for xylogenesis in conifers of cold climates. *Glob. Ecol. Biogeogr.* **2008**, *17*, 696–707. [[CrossRef](#)]
50. Moser, L.; Fonti, P.; Büntgen, U.; Esper, J.; Luterbacher, J.; Franzen, J.; Frank, D. Timing and duration of European larch growing season along altitudinal gradients in the Swiss Alps. *Tree Physiol.* **2010**, *30*, 225–233. [[CrossRef](#)] [[PubMed](#)]
51. Vieira, J.; Rossi, S.; Campelo, F.; Freitas, H.; Nabais, C. Xylogenesis of *Pinus pinaster* under a Mediterranean climate. *Ann. For. Sci.* **2014**, *71*, 71–80. [[CrossRef](#)]
52. Gruber, A.; Baumgartner, D.; Zimmermann, J.; Oberhuber, W. Temporal dynamic of wood formation in *Pinus cembra* along the alpine treeline ecotone and the effect of climate variables. *Trees* **2009**, *23*, 623–635. [[CrossRef](#)] [[PubMed](#)]
53. Liu, X.; Nie, Y.; Luo, T.; Yu, J.; Shen, W.; Zhang, L. Seasonal Shift in Climatic Limiting Factors on Tree Transpiration: Evidence from Sap Flow Observations at Alpine Treelines in Southeast Tibet. *Front. Plant Sci.* **2016**, *7*, 1018. [[CrossRef](#)] [[PubMed](#)]
54. Mellander, P.-E.; Bishiop, K.; Lundmark, T. The influence of soil temperature on transpiration: A plot scale manipulation in a young Scots pine stand. *For. Ecol. Manag.* **2004**, *195*, 15–28. [[CrossRef](#)]
55. Tian, Q.; He, Z.; Xiao, S.; Peng, X.; Ding, A.; Lin, P. Response of stem radial growth of Qinghai spruce (*Picea crassifolia*) to environmental factors in the Qilian Mountains of China. *Dendrochronologia* **2017**, *44*, 76–83. [[CrossRef](#)]
56. Duan, J.P.; Zhang, Q.B.; Lv, L.X.; Zhang, C. Regional-scale winter-spring temperature variability and chilling damage dynamics over the past two centuries in southeastern China. *Clim. Dyn.* **2012**, *39*, 919–928. [[CrossRef](#)]
57. Beedlow, P.A.; Lee, E.H.; Tingey, D.T.; Waschmann, R.S.; Burdick, C.A. The importance of seasonal temperature and moisture patterns on growth of Douglas-fir in western Oregon, USA. *Agric. For. Meteorol.* **2013**, *169*, 174–185. [[CrossRef](#)]

58. Li, X.X.; Liang, E.Y.; Gričar, J.; Prislan, P.; Rossi, S.; Čufar, K. Age dependence of xylogenesis and its climatic sensitivity in Smith fir on the south-eastern Tibetan Plateau. *Tree Physiol.* **2012**, *33*, 48–56. [[CrossRef](#)] [[PubMed](#)]
59. Prislan, P.; Gričar, J.; de Luis, M.; Smith, K.T.; Čufar, K. Phenological variation in xylem and phloem formation in *Fagus sylvatica* from two contrasting sites. *Agric. For. Meteorol.* **2013**, *180*, 142–151. [[CrossRef](#)]
60. Begum, S.; Nakaba, S.; Oribe, Y.; Kubo, T.; Funada, R. Induction of cambial reactivation by localized heating in a deciduous hardwood Hybrid Poplar (*Populus sieboldii* × *P. grandidentata*). *Ann. Bot.* **2007**, *100*, 439–447. [[CrossRef](#)] [[PubMed](#)]
61. Deslauriers, A.; Huang, J.G.; Balducci, L.; Beaulieu, M.; Rossi, S. The contribution of carbon and water in modulating wood formation in black spruce saplings. *Plant Physiol.* **2016**, *170*, 2072–2084. [[CrossRef](#)] [[PubMed](#)]
62. Gričar, J.; Zupančič, M.; Čufar, K.; Oven, P. Regular cambial activity and xylem and phloem formation in locally heated and cooled stem portions of Norway spruce. *Wood Sci. Technol.* **2007**, *41*, 463–475. [[CrossRef](#)]
63. Lenz, A.; Hoch, G.; Körner, C. Early season temperature controls cambial activity and total tree ring width at the alpine treeline. *Plant Ecol. Divers.* **2013**, *6*, 365–375. [[CrossRef](#)]
64. Antonova, G.; Stasova, V. Effects of environmental factors on wood formation in Scotts pine stems. *Trees* **1993**, *7*, 214–219. [[CrossRef](#)]
65. Vaganov, E.A.; Hughes, M.K.; Shashkin, A.V. Environmental control of xylem differentiation. In *Growth Dynamics of Conifer Tree Rings: Images of Past and Future Environments*; Vaganov, E.A., Hughes, M.K., Shashkin, A.V., Eds.; Springer: Berlin/Heidelberg, Germany, 2006; pp. 151–187.
66. Brooks, A.; Farquhar, G.D. Effect of temperature on the CO<sub>2</sub>/O<sub>2</sub> specificity of ribulose-1,5-bisphosphate carboxylase/oxygenase and the rate of respiration in the light. *Planta* **1985**, *165*, 397–406. [[CrossRef](#)] [[PubMed](#)]
67. Lewis, J.D.; Olszyk, D.; Tingey, D.T. Seasonal patterns of photosynthetic light response in Douglas-fir seedlings subjected to elevated atmospheric CO<sub>2</sub> and temperature. *Tree Physiol.* **1999**, *19*, 243–252. [[CrossRef](#)] [[PubMed](#)]
68. Steppe, K.; De Pauw, D.J.W.; Lemeur, R.; Vanrolleghem, P.A. A mathematical model linking tree sap flow dynamics to daily stem diameter fluctuations and radial stem growth. *Tree Physiol.* **2006**, *26*, 257–273. [[CrossRef](#)] [[PubMed](#)]
69. Zweifel, R.; Zimmermann, L.; Zeugin, F.; Newbery, D.M. Intra-annual radial growth and water relations of trees: Implications towards a growth mechanism. *J. Exp. Bot.* **2006**, *57*, 1445–1459. [[CrossRef](#)] [[PubMed](#)]
70. Shi, J.; Li, J.; Zhang, D.; Zheng, J.; Shi, S.; Ge, Q.; Lee, H.; Zhao, Y.; Zhang, J.; Lu, H. Two centuries of April–July temperature change in southeastern China and its influence on grain productivity. *Sci. Bull.* **2017**, *62*, 40–45. [[CrossRef](#)]
71. Cai, Q.F.; Liu, Y.; Duan, B.C.; Sun, C.F. Regional difference of the start time of the recent warming in Eastern China: Prompted by a 165-year temperature record deduced from tree rings in the Dabie Mountains. *Clim. Dyn.* **2017**, *50*, 2157–2168. [[CrossRef](#)]
72. Zheng, Y.; Shao, X.; Lu, F.; Li, Y. February–May temperature reconstruction based on tree-ring widths of *Abies fargesii* from the Shennongjia area in central China. *Int. J. Biometeorol.* **2016**, *60*, 1175–1181. [[CrossRef](#)] [[PubMed](#)]
73. Li, Y.; Fang, K.; Cao, C.; Li, D.; Zhou, F.; Dong, Z.; Zhang, Y.; Gan, Z. A tree-ring chronology spanning 210 years in the coastal area of southeastern China, and its relationship with climate change. *Clim. Res.* **2016**, *67*, 209–220. [[CrossRef](#)]
74. Zhao, Y.; Shang, Z.; Wang, J.; Guo, H.; Zhou, D.; Ding, M. Regional disparities about the relationships between tree-ring width of *Pinus massoniana* Lamb. and climatic factors: A case study in Jiuling Mountain and Jiulian Mountain. *J. Subtrop. Resour. Environ.* **2014**, *9*, 1–8.
75. Zhao, Y.; Shi, J.; Shi, S.; Wang, B.; Yu, J. Summer climate implications of tree-ring latewood width: A case study of *Tsuga longibracteata* in South China. *Asia Geogr.* **2017**, *34*, 131–146. [[CrossRef](#)]

76. Huang, J.; Bergeron, Y.; Zhang, L.; Denneler, B. Variation in intra-annual radial growth (xylem formation) of *Picea mariana* (Pinaceae) along a latitudinal gradient in western Quebec, Canada. *Am. J. Bot.* **2011**, *98*, 792–800. [[CrossRef](#)] [[PubMed](#)]
77. Su, J.; Gou, X.; Deng, Y.; Zhang, R.; Liu, W.; Zhang, F.; Lu, M.; Chen, Y.; Zheng, W. Tree growth response of *Fokienia hodginsii* to recent climate warming and drought in southwest China. *Int. J. Biometeorol.* **2017**, *61*, 2085–2096. [[CrossRef](#)] [[PubMed](#)]



© 2018 by the authors. Licensee MDPI, Basel, Switzerland. This article is an open access article distributed under the terms and conditions of the Creative Commons Attribution (CC BY) license (<http://creativecommons.org/licenses/by/4.0/>).